

## Modulation of Ligand Binding by Alternative Splicing of the $\alpha$ PS2 Integrin Subunit

Thomas A. Bunch,<sup>1\*</sup> Timmy L. Kendall,<sup>1</sup> Kishore Shakalya,<sup>2</sup> Daruka Mahadevan,<sup>2</sup> and Danny L. Brower<sup>1,3</sup>

<sup>1</sup>Department of Molecular and Cellular Biology, Arizona Cancer Center, 1515 N. Campbell Ave., Tucson, Arizona 85724

<sup>2</sup>Department of Medicine, Arizona Cancer Center, 1515 N. Campbell Ave., Tucson, Arizona 85724

<sup>3</sup>Department of Biochemistry, Arizona Cancer Center, 1515 N. Campbell Ave., Tucson, Arizona 85724

**Abstract** The *Drosophila*  $\alpha$ PS2 integrin subunit is found in two isoforms.  $\alpha$ PS2C contains 25 residues not found in  $\alpha$ PS2m8, encoded by the alternative eighth exon. Previously, it was shown that cells expressing  $\alpha$ PS2C spread more effectively than  $\alpha$ PS2m8 cells on fragments of the ECM protein Tigrin, and that  $\alpha$ PS2C-containing integrins are relatively insensitive to depletion of  $\text{Ca}^{2+}$ . Using a ligand mimetic probe for Tigrin affinity (TWOW-1), we show that the affinity of  $\alpha$ PS2C $\beta$ PS for this ligand is much higher than that of  $\alpha$ PS2m8 $\beta$ PS. However, the two isoforms become more similar in the presence of activating levels of  $\text{Mn}^{2+}$ . Modeling indicates that the exon 8-encoded residues replace the third  $\beta$  strand of the third blade of the  $\alpha$  subunit  $\beta$ -propeller structure, and generate an exaggerated loop between this and the fourth strand.  $\alpha$ PS2 subunits with the extra loop structure but with an m8-like third strand, or subunits with a C-like strand but an m8-like short loop, both fail to show  $\alpha$ PS2C-like affinity for TWOW-1. Surprisingly, a single C > m8-like change at the third strand-loop transition point is sufficient to make  $\alpha$ PS2C require  $\text{Ca}^{2+}$  for function, despite the absence of any known cation binding site in this region. These data indicate that alternative splicing in integrin  $\alpha$  subunit extracellular domains may affect ligand affinity via relatively subtle alterations in integrin conformation. These results may have relevance for vertebrate  $\alpha 6$  and  $\alpha 7$ , which are alternatively spliced at the same site. *J. Cell. Biochem.* 102: 211–223, 2007.

© 2007 Wiley-Liss, Inc.

**Key words:** cell adhesion; integrin structure–function; integrin alternative splicing; integrin  $\alpha 7$

Integrins are the primary family of receptors through which metazoan cells interact with the extracellular matrix, although some integrins bind directly to other cell surface molecules [Hynes, 2002]. Integrins are heterodimers of  $\alpha$  and  $\beta$  subunits, whose overall structures are highly conserved phylogenetically [Burke, 1999; Hynes and Zhao, 2000]. This conservation

likely is a result of constraints that are related to the remarkable concerted conformational changes that characterize the cellular regulation of integrin function, and integrin signaling events that follow ligand binding. Changes in integrin shape were originally demonstrated by a number of conformation-specific antibodies. More recently X-ray data from fragments of integrins, along with electron microscopic characterizations of different conformations, have permitted more precise interrogation of the integrin structure–function relationships [Xiong et al., 2001, 2002, 2003; Beglova et al., 2002; Takagi et al., 2002; Luo et al., 2003; Mould and Humphries, 2004; Springer and Wang, 2004; Luo and Springer, 2006]. An overall picture is emerging of a globular headpiece, with the  $\alpha$  and  $\beta$  components of the ligand binding site connected to the transmembrane domains by relatively long stalks. The stalks may be bent when the receptors are relatively inactive, and extended upon cellular activation. The headpieces also may sample relative high and low

This article contains supplementary material, which may be viewed at the Journal of Cellular Biochemistry website at <http://www.interscience.wiley.com/jpages/0730-2312/suppmat/index.html>.

Grant sponsor: NIH to DLB; Grant number: R01GM42474; Grant sponsor: The American Cancer Society to DM; Grant number: 5P30CA023074.

\*Correspondence to: Thomas A. Bunch, Arizona Cancer Center, Room 0977, 1515 N. Campbell Ave., Tucson, AZ 85724. E-mail: [tbunch@email.arizona.edu](mailto:tbunch@email.arizona.edu)

Received 21 November 2006; Accepted 9 January 2007

DOI 10.1002/jcb.21288

© 2007 Wiley-Liss, Inc.

ligand affinity states (often referred to as “head open” and “head closed”), which are thought to be driven, at least in part, by changes in the tertiary structure of the  $\beta$  subunit head. Although molecular interactions are being uncovered that influence these transitions, it appears that integrin dynamics are dictated by a complex set of relatively weak interactions, and we are only beginning to understand these. Moreover, there is a growing appreciation that integrin “activation” may involve an increasingly complex set of conformations and affinity states [Jin et al., 2004; Mould and Humphries, 2004; Litvinov et al., 2005; Luo and Springer, 2006].

Integrin function may be regulated by a host of cellular proteins, depending on the cell type [Liu et al., 2000]. Structural variations also influence integrin function, as evidenced by the large families of  $\alpha$  and  $\beta$  subunits in vertebrates. Within a single integrin gene, alternative splicing contributes to functional variety. However, alternative splicing affecting the extracellular domains is uncommon in vertebrates, with changes in a single region of  $\alpha 6$  and  $\alpha 7$  being the only well-characterized examples [de Melker and Sonnenberg, 1999]. Alternative splicing is more common in the fruit fly, *Drosophila melanogaster*, where the number of different subunit genes is much smaller than in vertebrates. Splicing variants altering extracellular domains have been found for each of the three well-characterized *Drosophila*  $\alpha$  subunits, as well as the primary fly  $\beta$  subunit [Brower, 2003].

The *Drosophila*  $\alpha$ PS2 subunit, with  $\beta$ PS, comprises the primary insect integrin of the “RGD binding” class.  $\alpha$ PS2 $\beta$ PS is expressed on many tissues throughout fly development, and genetic and cell biological studies have defined numerous morphogenetic functions for the receptor, associated with both adhesive and probably signaling requirements [Brown et al., 2000].  $\alpha$ PS2 is found in two isoforms [Brown et al., 1989], a canonical (“C”) form, and a version that is smaller by 25 amino acids, because it is missing exon 8 (“m8”). The ligand binding head of  $\alpha$  subunits is comprised of a  $\beta$  propeller structure with seven blades, each comprised of four strands of  $\beta$  sheet [Xiong et al., 2001]. The top of the propeller associates with the  $\beta$  subunit, and the bottom contains four potential cation binding sites. The residues encoded by  $\alpha$ PS2 exon 8 are inserted into the

third  $\beta$  propeller blade in the primary sequence, which is the same location as the alternative splices in human  $\alpha 6$  and  $\alpha 7$  [Graner et al., 1998; de Melker and Sonnenberg, 1999]. This location has potential to affect ECM ligand contact sites directly, or could affect function indirectly by altering conformation.

No  $\alpha$ PS2 isoform-specific antibodies have been developed; however the developmental distributions of the two forms were characterized by assaying the relative frequencies of cDNAs from different tissues [Brown et al., 1989]. In general,  $\alpha$ PS2C is most common in morphogenetically stable tissues, while  $\alpha$ PS2m8 predominates during dynamic developmental stages, such as during early embryogenesis and in larval imaginal disks. The cell biology of  $\alpha$ PS2 variants has also been investigated in cell culture, using cell shape and adhesion on defined ECM proteins as an assay [Zavortink et al., 1993; Graner et al., 1998]. These studies show that  $\alpha$ PS2C is superior to  $\alpha$ PS2m8 on ECM ligands such as Tiggrin, which is found at the strong adhesions at muscle attachment sites, and Ten-m. However,  $\alpha$ PS2m8 is somewhat better than  $\alpha$ PS2C on some ligands, such as an RGD-containing fragment of the fly laminin  $\alpha 1$ , 2 chain. These studies suggested the possibility that exon 8-encoded residues may contribute to a specific ligand binding surface. However, the potential for more global structural differences were suggested by the observation that  $\alpha$ PS2C and  $\alpha$ PS2m8 display qualitatively different cation requirements, with the former supporting cell spreading in the complete absence of extracellular  $\text{Ca}^{2+}$  [Zavortink et al., 1993].

Recently, we developed a ligand mimetic Fab for  $\alpha$ PS2 $\beta$ PS integrins [Bunch et al., 2006]. TWOW-1 was generated by cloning 53 residues (including the RGD motif) of Tiggrin into the H-CDR3 of the  $\alpha$ V $\beta$ 3 ligand mimetic WOW-1 [Pampori et al., 1999]. TWOW-1 binding to  $\alpha$ PS2 $\beta$ PS is rapid, reversible, inhibited by EDTA, dependent on the integrity of the ligand RGD motif, and sensitive to both activating and inactivating mutations in  $\alpha$ PS $\beta$ PS. Thus, TWOW-1 can be used to assay  $\alpha$ PS2 $\beta$ PS affinity for Tiggrin. Here, we have re-examined the functional differences of  $\alpha$ PS2C and  $\alpha$ PS2m8, including a new series of mutants to further define regions important for PS2 integrin–Tiggrin interactions. These studies also make use of modeling based on more recent structural

data for integrin subunits, as well as phylogenetic comparisons to indicate critical sequence motifs.

## METHODS

### Structural Modeling

Homology models of  $\alpha$ PS2m8 and  $\alpha$ PS2C were generated by threading insect sequences onto the X-ray crystal structure coordinates of human  $\alpha$ V $\beta$ 3 (1JV2) [Xiong et al., 2001]. Various models were built including some comprising the whole protein, the  $\alpha$ -subunit  $\beta$ -propeller domain alone, or this in combination with the  $\beta$ -subunit A/I domain. Modeller (version 7) was used for homology modeling of aligned sequences and then superimposed (homology aligned using Sybyl 7.2) on the original crystal structure and merged into a single coordinate file after removing the  $\alpha$ V structural coordinates. The models were energy minimized using Sybyl 7.2. For  $\alpha$ PS2C initial models of the extra loop structures were problematical, perhaps due to the high proline content in this region. To solve this, we first modeled  $\alpha$ PS2C from the mosquito *Anopheles gambiae*, and subsequently used this as an initial template for *D. melanogaster*  $\alpha$ PS2C. (Although no cDNA sequence was available for the mosquito, one was constructed from genomic sequences.)

The proline-rich exon 8 region insertion GQTYSIPDAKFPFKPPLYQPFGTG was built by Modeller as a distorted  $\alpha$ -helix. Since proline-rich regions are not  $\alpha$ -helical we checked the phi-psi angles of the residues in this segment. To change the phi-psi angles, one residue on either side of each proline was extracted and the phi-psi angles were changed to match an ideal collagen-like polyproline helix. A local energy minimization was performed for a region of around 5 Å incorporating the four prolines in Sybyl 7.2. The final model was superimposed on the original model to obtain a root mean square deviation of <1 Å. For details, see the Supplementary Materials.

### PS Integrin Constructs

$\alpha$  and  $\beta$  subunits were expressed from pHS $\beta$ PS4A, pHS $\alpha$ PS2C, pHS $\alpha$ PS2m8, and variants of these [Bunch and Brower, 1992]. Mutations of the  $\alpha$ PS2 genes were introduced into pHS $\alpha$ PS2C and pHS $\alpha$ PS2m8 using standard PCR and molecular biology protocols.

Regions mutated and those generated by PCR were sequenced to verify changes and to ensure that no unintended mutations had been introduced.

### Cell Culture and Transfection

*Drosophila* S2/M3 were cultured in Shields and Sang M3 medium supplemented with 12% heat-inactivated fetal calf serum as previously described [Bunch and Brower, 1992]. Cells were cotransfected with plasmids expressing a  $\beta$ PS subunit and an  $\alpha$ PS2 subunit (either pHS $\alpha$ PS2m8, pHS $\alpha$ PS2C, or their variants), both under the regulation of the heat shock protein 70 promoter, and with the bacterial DHFR selectable marker (plasmid p8HCO) as described [Jannuzi et al., 2002]. For transient expression experiments, the day after transfection the medium was replaced with selection medium containing  $2 \times 10^{-7}$  M methotrexate and the cells were allowed to grow for an additional 2 days prior to TWOW-1 binding assays.

### TWOW-1 Binding Assays

The TWOW-1 binding assay was done as initially described [Bunch et al., 2006] with the following modifications. To obtain more similar expression levels we have used transiently transfected cells. In this paradigm the cells express high levels of integrins in the first few days in the absence of heat shock; therefore, we did not heat shock the cells. Also, we did not protease-clear the cells as the transiently transfected cells do not quickly replace the cleared integrins following their removal. Because we examined only variants of the  $\alpha$ PS2 subunit we did not remove endogenous  $\beta$ PS subunits by treating the cells with RNAi targeting the endogenous *myspheroid* gene. Our S2 cells express little, if any,  $\alpha$ PS2 integrin subunits and bind no TWOW-1 in the absence of transfected  $\alpha$ PS2 genes [Bunch et al., 2006]. Finally, the first wash of the EDTA-treated cells with BES-Tyrodes containing EDTA was found to be unnecessary. These cells therefore were simply washed in BES-Tyrodes prior to the TWOW-1 binding assay.

The TWOW-1 binding was assessed by flow cytometry as described [Bunch et al., 2006].  $1 \times 10^6$  cells were washed with BES-Tyrodes and resuspended in 30  $\mu$ l BES-Tyrodes supplemented with 1 mg/ml (w/v) BSA, 1.66 mM

MgCl<sub>2</sub>, and 16.6 μM CaCl<sub>2</sub>. In some cases, 1.66 mM MnCl<sub>2</sub> was included in this buffer to activate the integrin. To assess the dependency of TWOW-1 binding on Ca<sup>2+</sup> we resuspended the cells in 1.66 mM MgCl<sub>2</sub> and 0.41 mM EGTA. To assess non-specific TWOW-1 binding, cells were resuspended in 30 μl BES-Tyrodes containing 1 mg/ml BSA and 16.6 mM EDTA. Binding assays were initiated by adding 20 μl of TWOW-1 at a concentration of 300 μg/ml (in BES-Tyrodes) for 10 min at room temperature. Fifty μl of 4% formaldehyde in BES-Tyrodes was added to fix the bound TWOW-1 to the cells, and after 5 min of fixation 1.5 ml BES-Tyrodes was added, cells were spun down and resuspended for 25 min on ice in 100 μl BES-Tyrodes (+1 mg/ml BSA) containing 20 μg/ml AlexaFluor488 goat anti-mouse IgG (Molecular Probes, A-11029) and 10 μg/ml R-Phycoerythrin labeled streptavidin (Molecular Probes, S-866). The R-Phycoerythrin-streptavidin was used to detect and exclude from analysis cells that had been disrupted. After incubation with secondary antibody, the cells were spun down and resuspended in 250 μl PBS followed by immediate addition of 250 μl of 4% formaldehyde in PBS to fix the secondary antibody; the cells were assayed in the flow cytometer in this solution.

Levels of αPS2 integrin on the surface of cells were determined by staining with the biotin labeled anti-αPS2 antibody CF.2C7 (which is not conformation specific) as described [Bunch et al., 2004].  $5 \times 10^5$  cells were incubated for 25 min at room temperature in 50 μl of biotinylated CF.2C7 in M3 + 12.5% FCS. Then R-Phycoerythrin-streptavidin diluted in M3 + FCS was added to a final concentration of 10 μg/ml and incubated for an additional 30 min on ice. Cells were fixed by the addition of 0.5 ml 2% formaldehyde in PBS. Other experiments determined that both antibody and streptavidin were present at saturating levels. Fluorescence levels for both TWOW-1 and αPS2 levels were analyzed by flow cytometry at the ARL-Biotechnology Cell Sorting Facility at the University of Arizona.

Specific TWOW-1 binding was measured as mean fluorescence intensity (MFI) minus the TWOW-1 MFI of the same cells in the presence of EDTA. For our analyses, this specific binding is expressed relative to surface integrin expression (TWOW-1 MFI/anti-αPS2 MFI).

### Cell Spreading

The ligand for cell spreading experiments was RBB-Tigg, a bacterial fusion protein that contains the same 53 amino acids of Tiggrin that are found in TWOW-1 (residues 1964–2016, including the RGD sequence of Tiggrin and 25 amino acids upstream and downstream), fused to a histidine tag, from the pTrcHisB vector [Bunch et al., 2004]. 96-well tissue culture plates were coated with 50 μl RBB-Tigg (0.5 μg/ml in PBS) overnight at 4°C, then blocked with 20% dried milk in PBS for 1 h at room temperature, and washed 3× with PBS.

Transiently transfected cells were rinsed in BES-Tyrodes and then diluted to  $2 \times 10^5$ /ml in BES-Tyrodes containing 1 mg/ml BSA (w/v), 1 mM MgCl<sub>2</sub>, and 10 μM CaCl<sub>2</sub> or the same lacking CaCl<sub>2</sub> and containing 0.25 mM EGTA. One hundred μl of cells were allowed to spread for 1 h and then fixed by the addition of an equal volume of 4% formaldehyde in BES-Tyrodes. Photographs were obtained using a Nikon Coolpix 5000 camera attached to a Nikon phase-contrast microscope (Nikon Diaphot-TMD).

## RESULTS

### Modeling αPS2 Structures

At the time of the last investigation of αPS2 isoforms the best model for the structure of the integrin α subunit head was the seven bladed β-propeller, based on secondary structure predictions [Springer, 1997]. Sequence alignments predicted that the exon 8 residues specific to αPS2C inserted before the third β sheet strand of the third blade of the propeller [Graner et al., 1998]. One possibility is that the new residues form a novel structure between strands 2 and 3 of the blade. In this case the novel addition would be near regions thought important for ligand association, and also near the α/β interface. Alternatively, the exon 8-encoded amino acids could replace the third β sheet strand, and create an extended connection between strands 3 and 4 at the back of the β-propeller. Secondary structural predictions at the time were consistent with either possibility. The determination of high resolution X-ray data for the β-propeller region of human αV and αIIb [Xiong et al., 2001, 2002; Xiao et al., 2004] allowed us to build models for the β-propeller of αPS2 isoforms, using threading algorithms and energy minimization considerations. As expected from the

sequence, the models predict that for  $\alpha$ PS2m8 the loop connecting the third and fourth  $\beta$  strands of blade 3 is short compared to that found in  $\alpha$ V (Fig. 1A). When exon 8 is included, the models indicate that the MASS sequence motif that forms the third blade, third  $\beta$  sheet

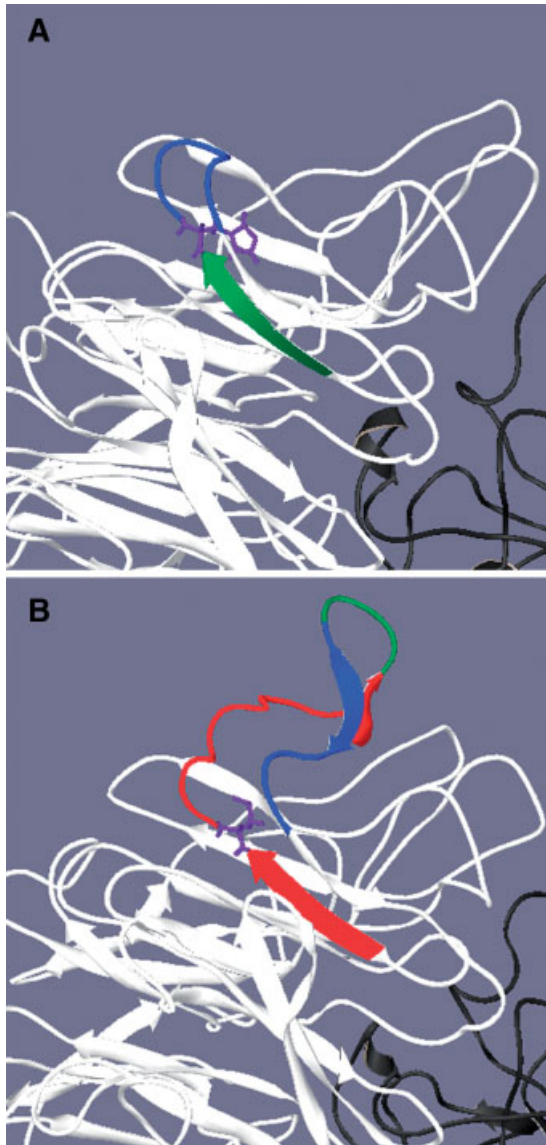


**Fig. 1.** Models of  $\alpha$ PS2m8 (top) and  $\alpha$ PS2C (bottom), generated primarily by threading sequences through the X-ray structure for  $\alpha$ V $\beta$ 3 [Xiong et al., 2001]. The sequences comprising the third  $\beta$  strand of the third blade of the  $\alpha$ PS2  $\beta$ -propeller in  $\alpha$ PS2m8 are in green, with the loop connecting this to the fourth  $\beta$  strand in blue. Modeling consistently indicates that these residues are displaced in  $\alpha$ PS2C, where exon 8-encoded residues (red) now comprise the third  $\beta$  strand, and contribute to an extended loop structure. In each panel, the residue at the end of the third strand is in violet (histidine in  $\alpha$ PS2m8, isoleucine in  $\alpha$ PS2C); see text for discussion of the importance of this residue.  $\beta$ PS structures are black.

strand in  $\alpha$ PS2m8 is replaced by QTYs encoded by the beginning of exon 8. The rest of the exon and the beginning of exon 9 then create a larger loop at the back of the  $\beta$  propeller before connecting to the fourth  $\beta$  sheet strand, which is unchanged. The larger loop includes a collagen-like polyproline helix at the top and back (away from the  $\beta$  subunit I domain) of the  $\alpha$ PS2C  $\beta$ -propeller (Fig. 1B). Although some of our models have differed in the conformation of this extended loop, no predicted structure has resulted in which a new loop is created in  $\alpha$ PS2C on the side facing the  $\beta$  subunit; in every case the first exon 8-encoded residues replace the third  $\beta$  strand of the third blade of the  $\beta$ -propeller.

The conclusion that exon 8 encodes a new strand of  $\beta$  sheet is further supported by sequence comparisons of  $\alpha$ PS2 from other insects. In *D. melanogaster* the purported sequences of this strand are not highly similar (MASS in  $\alpha$ PS2m8, QTYs in  $\alpha$ PS2C). We searched the genomic sequence data for other insects, looking for potential “exon 8s” in their  $\alpha$ PS2 genes (Fig. 2). The putative strand sequences are more similar in some other Drosophilids, and much more so in three other

Dmel	<u>GQ</u> TYSIPPDAKFFPKPPLYQP-FGTG	<u>GM</u> ASSHDVTRPENQVFST
Dslm	<u>GQ</u> TYSIPPDAEFPFKPPLYQP-FGTG	<u>GM</u> ASSHDVTRPENQVFST
Dsech	<u>GQ</u> IYSIPPDAMFFPKPPLYQP-FGTG	<u>GM</u> ASSHDVTRPENQVFST
Dyak	<u>GQ</u> TYSIPPDAKFFPKPPLYQP-FGTG	<u>GM</u> ASSHDVTRPENQVFST
Dere	<u>GQ</u> TYSIPPDAEFPFKPPLYQP-FGTG	<u>GM</u> ASSHDVTRPENQVFST
Dana	<u>GQ</u> TYSIPPDAEFPFKPPYQP-FGTG	<u>GQ</u> ASSHDVTRPENQVFST
Dpers	<u>GQ</u> TYSIPPDAEFPFKPPYQP-FGTG	<u>GQ</u> ASSHDVTKPENQVFST
Dpse	<u>GQ</u> TYSIPPDAEFPFKPPYQP-FGTG	<u>GQ</u> ASSHDVTKPENQVFST
Dwil	<u>GE</u> TYSIPPDAEFPFKPPYQP-FGTG	<u>GQ</u> ASSHDVTKPENQVFST
Dvir	<u>GQ</u> TYSIPPDAEFPFKPPYQP-FGTG	<u>GQ</u> AISSQDVTKPENQVFST
Dmoj	<u>GQ</u> TYSIPPDAEFPFKPPYQP-FGTG	<u>GQ</u> AISSQDVTKPENQVFST
Dgri	<u>GQ</u> TYSIPPDAEFPFKPPYQP-FGTG	<u>GQ</u> AISSQDVTKPENQVFST
Ccap	<u>GQ</u> AYSISPDAEFPFKPPYQP-FGTG	<u>GQ</u> TYSYDVTRPENQVYST
Agam	<u>GQ</u> MSINTDVVFPYKPPRYGH-FGEG	<u>GQ</u> IYSFSLNNPKDKVYKT
Aaeg	<u>GQ</u> VYSINTEAAFPYKPPRYGQ-FGEG	<u>GQ</u> IYSFSLNNPRDKVYST
Tcas	<u>GQ</u> MSVDAHATFEFKPTLFSATYGDE	<u>GQ</u> VHQQSLETRP-AVFAT

**Fig. 2.** Sequences of  $\alpha$ PS2 m8-C variants. Sequences of residues encoded by “exon 8” from various insects are on the left, with the corresponding “m8” residues on the right; an  $\alpha$ PS2C subunit includes both. The proposed third and fourth  $\beta$  strand sequences of the third blade of the  $\beta$ -propeller are underlined for the m8 residues. In  $\alpha$ PS2C the double underlining indicates residues that replace the m8 third strand residues in the structure. Note that the sequence divergence of these alternative strands is especially pronounced in *D. melanogaster* and its close relatives. Only some of these sequences have been confirmed by cDNAs, but genomic sequence is consistent with homologous alternative splicing in each of these species. *Drosophila* species in order are: *melanogaster*, *simulans*, *sechellia*, *yakuba*, *erecta*, *ananassae*, *persimilis*, *pseudoobscura*, *willistoni*, *virilis*, *mojavensis*, and *grimshaw*. *Ceratitis capitata* is the Mediterranean fruit fly, *Anopheles gambiae* and *Aedes aegypti* are mosquitoes, and *Tribolium castaneum* is a beetle.

dipterans. The difference appears to result from divergence in the  $\alpha$ PS2m8 sequence (MASS) in *D. melanogaster* and its close relatives. For example, in two genera of mosquitoes the  $\alpha$ PS2m8 strand (QIYS) is very similar to the proposed  $\alpha$ PS2C strand, which is QXYS in all cases examined. Thus, the “exon 8” insertions into the translated polypeptide would be expected to contribute to the  $\beta$  strand structure as easily as the  $\alpha$ PS2m8 sequence.

#### Ligand Affinity of $\alpha$ PS2 Isoforms

*Drosophila* S2 cells expressing  $\alpha$ PS2C $\beta$ PS spread on tissue culture plates coated with a fragment of the fly ECM protein Tigrin (RBB-Tigg).  $\alpha$ PS2m8 $\beta$ PS also mediates cell spreading on Tigrin and Tigrin fragments, but less effectively than  $\alpha$ PS2C $\beta$ PS [Zavortink et al., 1993; Graner et al., 1998]. The Fab TWOW-1 facilitates direct measurements of ligand affinity of  $\alpha$ PS2-containing integrins [Bunch et al., 2006]. Importantly for this study, TWOW-1 contains the same fragment of Tigrin as RBB-Tigg, which mediates cell spreading as effectively as full-length Tigrin on a molar basis, and displays similar  $\alpha$ PS2 isoform preferences [Fogerty et al., 1994; Graner et al., 1998; Jannuzi et al., 2002]. Thus, we expect that TWOW-1 contains all of the sites that interact directly with  $\alpha$ PS2 $\beta$ PS.

We quantitated TWOW-1 binding to cells expressing the two  $\alpha$ PS2 isoforms with  $\beta$ PS. (In all cases, values are expressed as a ratio of TWOW-1 bound divided by total  $\alpha$ PS2, determined by the binding of the monoclonal antibody CF.2C7. Previous work has shown that this ratio is not affected by integrin expression levels over a wide range.)  $\alpha$ PS2C $\beta$ PS binds TWOW-1 much more effectively than does  $\alpha$ PS2m8 $\beta$ PS (Fig. 3). The difference in binding of soluble TWOW-1 between isoforms is greater than the difference seen in the ability of the  $\alpha$ PS2 isoforms to mediate cell spreading on Tigrin fusion proteins; in this latter assay, the effectiveness of  $\alpha$ PS2m8 is at least 50% of the value for  $\alpha$ PS2C at all concentrations of Tigrin fusion proteins [Zavortink et al., 1993; Graner et al., 1998].

We next asked if the TWOW-1 binding capacities of the two isoforms are different, by assaying binding in the presence of activating concentrations of  $Mn^{2+}$ , a well-known activator of integrins generally, including  $\alpha$ PS2C $\beta$ PS [Bunch et al., 2006]. In the presence of  $Mn^{2+}$ ,

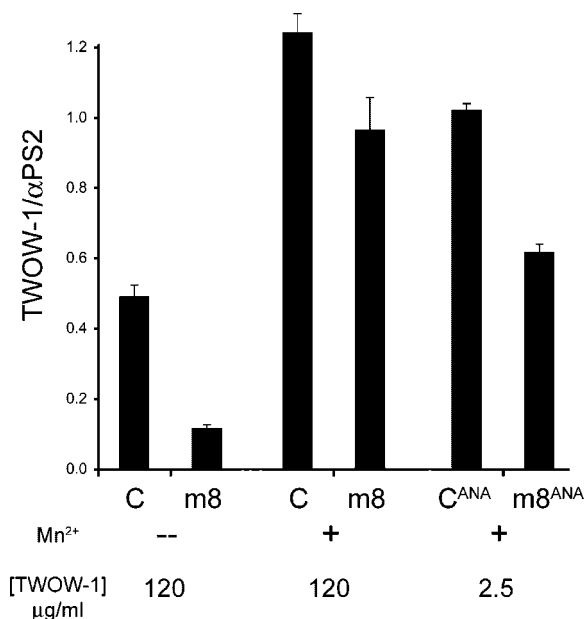


**Fig. 3.** Binding of the ligand mimetic TWOW-1 Fab/total  $\alpha$ PS2 for  $\alpha$ PS2m8 $\beta$ PS and  $\alpha$ PS2C $\beta$ PS on S2 cells.  $\alpha$ PS2C-containing integrins bind more than twice as well as  $\alpha$ PS2m8 integrins. In the presence of 1 mM activating  $Mn^{2+}$  ions both variants show higher and more similar affinity for ligand at high concentrations of TWOW-1, which saturate for activated  $\alpha$ PS2C $\beta$ PS.  $\alpha$ PS2C and  $\alpha$ PS2m8 integrin isoforms that are activated by both  $Mn^{2+}$  and a cytoplasmic mutation in  $\alpha$ PS2 (GFFNR > GFANA) were also tested at very low TWOW-1 concentrations (2.5  $\mu$ g/ml) that do not saturate for these high affinity receptors. Under these conditions, the apparent affinities of the isoforms are not equal, but they are more similar than for unactivated integrins. All values represent a minimum of three experiments; error bars equal the standard error.

TWOW-1 binding capacity increases for both  $\alpha$ PS2m8- and  $\alpha$ PS2C-containing integrins and the difference between the isoforms is greatly reduced (Fig. 3). At first glance this experiment might suggest that the differences between  $\alpha$ PS2C and  $\alpha$ PS2m8 result primarily from conformational changes; however the concentration of TWOW-1 used (120  $\mu$ g/ml) is above saturation levels for  $\alpha$ PS2C $\beta$ PS in the presence of  $Mn^{2+}$  [Bunch et al., 2006]. To get a better measure of the relative binding abilities of conformationally activated integrins, we tested receptors containing the activating cytoplasmic mutation GFFNR > GFANA in the presence of  $Mn^{2+}$ . In this experiment, we added TWOW-1 at 2.5  $\mu$ g/ml, which is below saturation (the binding plateau) of these hyperactivated integrins. Under these conditions, TWOW-1 binding to  $\alpha$ PS2C $\beta$ PS is still greater than that of  $\alpha$ PS2m8 $\beta$ PS, but the two isoforms are more

similar than under the original non-activating conditions ( $\alpha\text{PS2C}/\alpha\text{PS2m8} = 1.7$  vs 4.2 for normal cells at high TWOW-1; Fig. 3). Thus, much of the difference between PS2C and PS2m8 integrins' binding affinity for TWOW-1 can be removed as the integrins are activated to increasing degrees.

#### Are Critical Residues of $\alpha\text{PS2C}$ in the $\beta$ -Propeller Strand or the Extra Loop Structure?

The insertion of exon 8 adds a significant structure in the loop between two  $\beta$  sheet strands, and also changes the sequence in one of the strands. To ask if one or both of these alterations is important for the functional differences in  $\alpha\text{PS2}$  isoforms, we constructed a number of variants in this region (Fig. 4A; for all of the mutants, the initial m8 or C designation in the name refers to the form of the  $\beta$  strand at the beginning of the sequence). All of these were tested for TWOW-1 binding in the absence or presence of activating  $\text{Mn}^{2+}$  ions. The fact that all of the variants can bind high levels of TWOW-1 in the presence of  $\text{Mn}^{2+}$  (Fig. 4C) demonstrates that low affinity under normal conditions does not result from gross disruptions of the ligand binding capabilities of the mutants, for example, due to the elimination of a critical ligand interacting site. All of the mutants described here are expressed at levels similar to those of wild-type integrins.

We first eliminated most of the new loop residues with two largely overlapping deletions (C-del1 and C-del2), each of which leaves the  $\alpha\text{PS2C}$  sequence in the third  $\beta$  sheet strand. Both deletions bind TWOW-1 in amounts more similar to that found for  $\alpha\text{PS2m8}$ -containing integrins than  $\alpha\text{PS2C}$  (Fig. 4B). TWOW-1 binding to C-del2 is better than to  $\alpha\text{PS2m8}$ , but still less than half the value for  $\alpha\text{PS2C}$ -containing integrins. Thus, the extra loop residues are required to fully confer  $\alpha\text{PS2C}$ -like properties on integrin heterodimers. As can be seen from Figure 4A, the primary difference between the deletions is that C-del2 contains six residues at the beginning of the extra loop structure of  $\alpha\text{PS2C}$ .

To address the importance of the extra loop residues relative to the strand sequence in a different way, we made an  $\alpha\text{PS2}$  with the extra residues of  $\alpha\text{PS2C}$ , but with the potential  $\beta$ -propeller strand with the  $\alpha\text{PS2m8}$  sequence MASSHD. The TWOW-1 binding of integrins with this subunit ( $\alpha\text{PS2m8-C}$ ) is similar to that

of receptors with the C-del2 variant of  $\alpha\text{PS2}$ . That is, it is better than that seen for  $\alpha\text{PS2m8}$ , but much less than found for  $\alpha\text{PS2C}$ . Thus, the extra loop residues alone are not sufficient to confer  $\alpha\text{PS2C}$ -like properties on integrin heterodimers.

#### Detailed Analysis of the Proximal Loop Region

Comparison of the sequences and behaviors of the above mutants suggested that the sequence just after the end of the third strand of the third blade of the  $\beta$ -propeller might be a particularly critical region for distinguishing between  $\alpha\text{PS2m8}$  and  $\alpha\text{PS2C}$ . This suggestion is consistent with phylogenetic sequence comparisons (Fig. 2). The first residue after the end of the strand in all of the exon 8-encoded  $\alpha\text{PS2C}$  sequences is isoleucine (in the flies and mosquitoes) or valine (in the beetle). In  $\alpha\text{PS2m8}$  this residue is large and usually polar (histidine, glutamine, tyrosine, or in mosquitoes, phenylalanine). To examine this in more detail, we made a series of  $\alpha\text{PS2m8}$ - and  $\alpha\text{PS2C}$ -like subunits with changes in this region.

In the Drosophilids, the  $\beta$ -propeller strand of  $\alpha\text{PS2m8}$  extends to histidine or glutamine, followed by aspartate and valine; the corresponding sequence of  $\alpha\text{PS2C}$  is isoleucine-proline-proline (HDV vs IPP). We made two variants of  $\alpha\text{PS2m8}$  (Fig. 4A). In one, most of the short loop between the third and fourth  $\beta$ -propeller strands was replaced with the corresponding  $\alpha\text{PS2C}$  residues (m8-IPP+). In m8-IPP, only the HDV of  $\alpha\text{PS2m8}$  was replaced by the IPP sequence of  $\alpha\text{PS2C}$ , and m8-I contains a single H > I replacement. All of these display TWOW-1 affinities similar to or even slightly worse than those of integrins containing intact  $\alpha\text{PS2m8}$  (Fig. 4B). We also made variants of  $\alpha\text{PS2C}$  in which the IPP sequence was changed to HPP, IDP, or HDP (C-H, C-D, and C-HD, respectively). These mutants display TWOW-1 binding that is more similar to that found for  $\alpha\text{PS2C}$  integrins (Fig. 4B). The two variants in which histidine replaces isoleucine bind TWOW-1 slightly less well, whereas the C-D subunit binds at least as well as intact  $\alpha\text{PS2C}$  integrins. Thus, changing residues just after the end of the third strand of the third blade of the  $\beta$ -propeller can have relatively minor effects, but they are not sufficient to confer  $\alpha\text{PS2C}$ -like TWOW-1 binding properties on  $\alpha\text{PS2m8}$ , or vice versa.

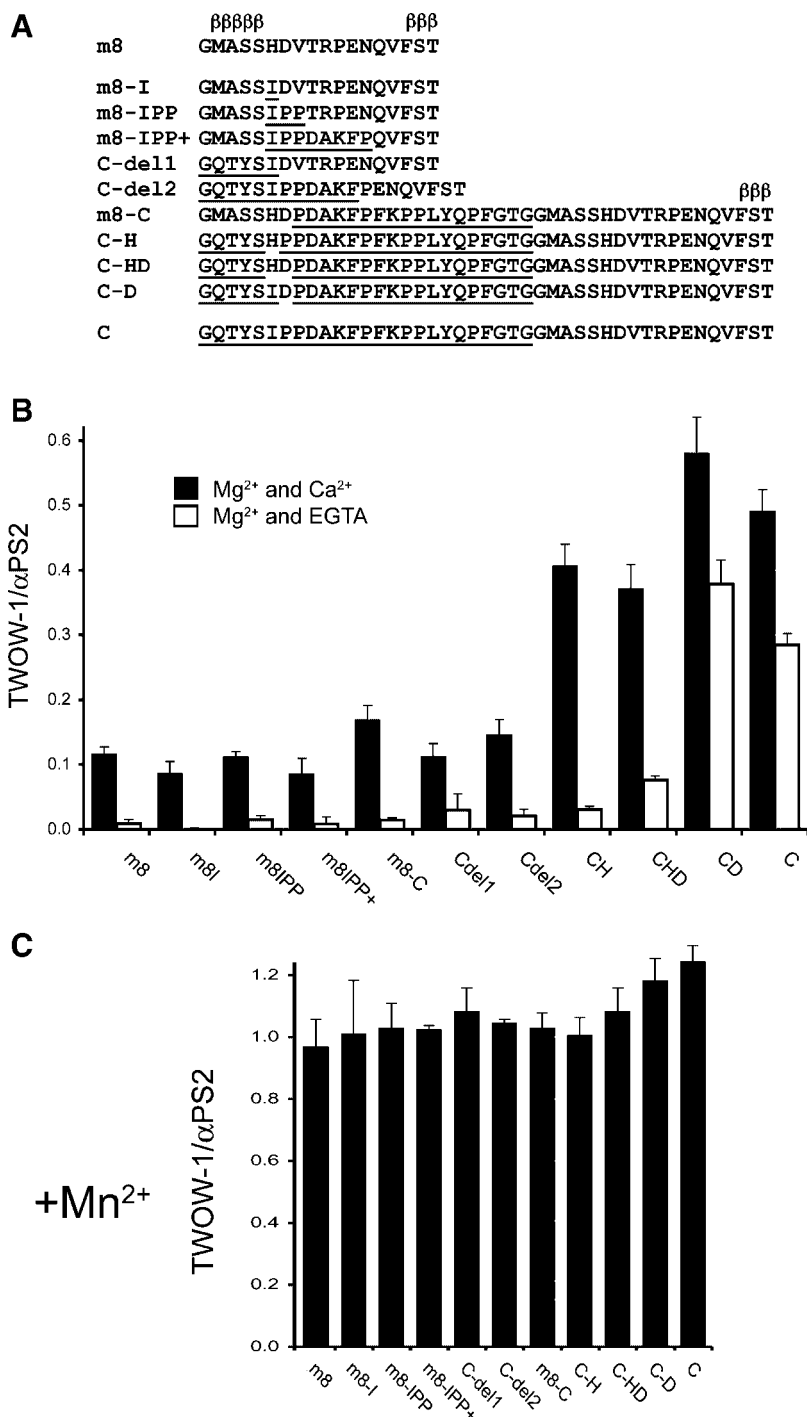


**Fig. 4.** **A:** Alternative sequences of  $\alpha$ PS2m8 (top) and  $\alpha$ PS2C (bottom), along with the variants constructed in this study. Residues typically encoded by exon 8 are underlined for each variant. As indicated by the “ $\beta$ ”s, modeling indicates that the sequences that contribute to the third  $\beta$  strand of the third blade of the  $\alpha$ PS2  $\beta$ -propeller structure immediately follow the first glycine, and the fourth  $\beta$  strand includes the FST motif. **B:** Binding of the ligand mimetic TWOW-1 (at 120  $\mu$ g/ml) Fab/total  $\alpha$ PS2 for  $\alpha$ PS2 $\beta$ PS variants on S2 cells. For each variant,

binding is shown in the presence of  $\text{Ca}^{2+}$  and  $\text{Mg}^{2+}$  (solid bars), and in  $\text{Mg}^{2+}$  with saturating concentrations of the  $\text{Ca}^{2+}$  chelator EGTA (open bars). **C:** All of the variants bind TWOW-1 in the presence of activating concentrations of  $\text{Mn}^{2+}$  ions (1 mM), demonstrating that the mutations do not directly compromise the ligand interacting sites. Note that the Y-axis is different from panel B. All values represent a minimum of three experiments; error bars equal the standard error.



### Ca<sup>2+</sup> Requirements

In our earlier cell spreading assay, we found that cells expressing  $\alpha$ PS2C $\beta$ PS were able to spread efficiently on fragments of Tiggrin in the absence of Ca<sup>2+</sup> (i.e., in the presence of EGTA), but  $\alpha$ PS2m8-containing integrins showed Ca<sup>2+</sup> ion dependence [Zavortink et al., 1993]. We assayed TWOW-1 binding for all of the mutants described here in the absence of Ca<sup>2+</sup> (i.e., in the presence of excess EGTA but with Mg<sup>2+</sup> present). As expected,  $\alpha$ PS2C integrins bind significant amounts of TWOW-1 in the absence of Ca<sup>2+</sup>, typically greater than 50% of the values in Ca<sup>2+</sup> and Mg<sup>2+</sup>, while  $\alpha$ PS2m8 shows a strong Ca<sup>2+</sup> requirement (Fig. 4B). Of the mutants, only C-D ( $\alpha$ PS2C with IPP changed to IDP) shows a Ca<sup>2+</sup> independence similar to  $\alpha$ PS2C, although for some others (C-del2, C-H, and C-HD) a very slight amount of TWOW-1 binding can be detected in the absence of Ca<sup>2+</sup>. Most significantly, changing a single residue in  $\alpha$ PS2C (the isoleucine immediately at the end of the third  $\beta$  sheet strand to the  $\alpha$ PS2m8 histidine) is sufficient to confer a Ca<sup>2+</sup> requirement for efficient  $\alpha$ PS2C $\beta$ PS ligand binding.

Ca<sup>2+</sup> sensitivity can be somewhat difficult to assay with soluble ligand binding assays for some variants; because  $\alpha$ PS2m8 $\beta$ PS binding to TWOW-1 is so low normally, measuring a decrease upon Ca<sup>2+</sup> depletion with EGTA might be unreliable. Therefore, we also examined Ca<sup>2+</sup> requirements in a cell spreading assay (Fig. 5, Table I), where wild-type  $\alpha$ PS2m8 performs well in Ca<sup>2+</sup> and Mg<sup>2+</sup>, but fails to support cell spreading in EGTA and Mg<sup>2+</sup> [Zavortink et al., 1993]. Cell spreading assays are influenced more by total integrin expression than is TWOW-1 binding (which is expressed as a ratio of TWOW-1 to total integrin), making quantitation less precise. However, even with this caveat, these experiments confirm the data for TWOW-1 binding; cells expressing integrins containing  $\alpha$ PS2C or the C-D variant spread well in medium depleted of Ca<sup>2+</sup>. All of the other variants display very slight spreading at most, including C-H, which contains the single residue replacement.

### DISCUSSION

Modeling strongly indicates that the new residues encoded by exon 8 replace the third  $\beta$  strand of the third blade of the  $\alpha$ PS2  $\beta$ -propeller, and lead to an exaggerated loop structure

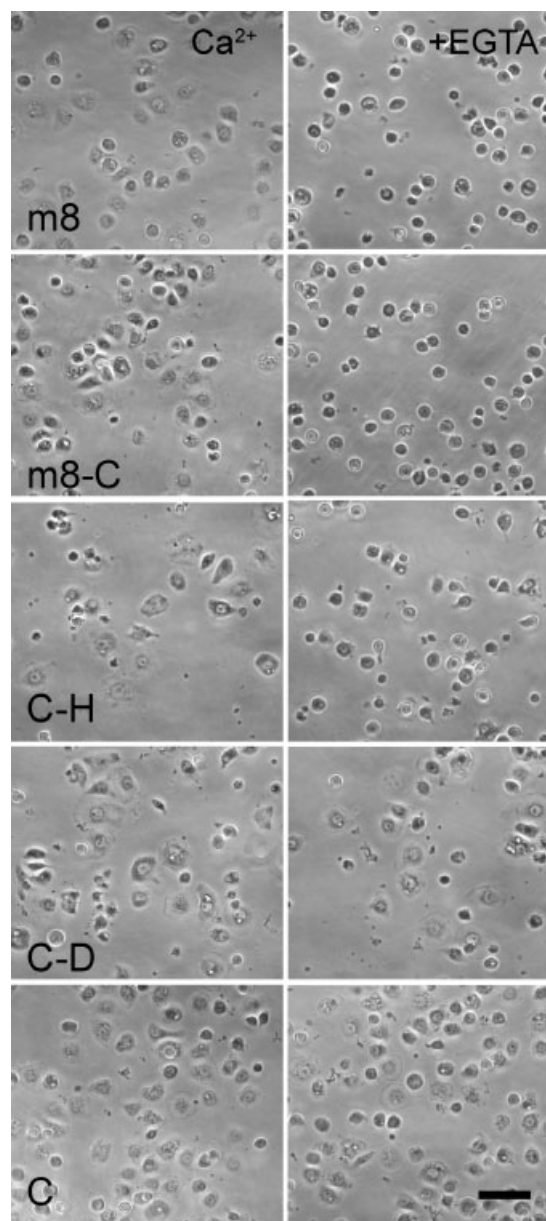


**Fig. 5.** Spreading on a fragment of the ECM protein Tigrin by S2 cells expressing variants of  $\alpha$ PS2 integrins. Integrins containing  $\alpha$ PS2m8,  $\alpha$ PS2C or any of the mutants tested will spread on plates coated with 0.5  $\mu$ g/ml RBB-Tigg in the presence of Ca<sup>2+</sup> and Mg<sup>2+</sup> (left column). However, when Ca<sup>2+</sup> is removed by the addition of EGTA (right column), significant spreading is observed only for cells expressing  $\alpha$ PS2C (bottom) or the  $\alpha$ PS2C-D variant, which also show efficient TWOW-1 binding in EGTA. Notably, the single substitution of a histidine for isoleucine in  $\alpha$ PS2C-H is sufficient to render these integrins Ca<sup>2+</sup> sensitive for spreading. Scale bar = 50  $\mu$ m.

between the third and fourth  $\beta$  strands. Two lines of evidence provide confirmation of the model. First, examination of the homologous sequences from closely related species reveals

**TABLE I. Quantitation of Cell Spreading Data from Experiments Illustrated in Figure 5**

	Cell spreading on RBB-Tigg	
	% Cells spread	
	+Ca <sup>2+</sup>	+EGTA
$\alpha$ PS2m8	61 ± 1	0 ± 0.2
$\alpha$ PS2m8-C	53 ± 6	1 ± 0.3
$\alpha$ PS2C-H	58 ± 6	1 ± 0.3
$\alpha$ PS2C-D	62 ± 5	50 ± 2
$\alpha$ PS2C	65 ± 3	65 ± 6

Spread cells were counted for three fields of each condition (minimum of 100 cells/field). Numbers represent means and standard error. The relatively high levels of spreading for  $\alpha$ PS2m8 integrins in the presence of Ca<sup>2+</sup> (essentially identical to  $\alpha$ PS2C integrins) are due to the high concentrations of ligand in these experiments. Even at these high RBB-Tigg levels, the Ca<sup>2+</sup> requirement of  $\alpha$ PS2m8 and similar mutants is clear.

not only structural homology but also sequence similarity between the putative third  $\beta$  strands in  $\alpha$ PS2C and  $\alpha$ PS2m8. More directly, the C-del1 and C-del2 mutations produce functional integrins even though both remove the sequences of the third blade of the  $\beta$ -propeller found in the  $\alpha$ PS2m8 integrin subunit. If the model is incorrect and exon 8 does not contain an alternative third  $\beta$  strand it is difficult to see how a functional integrin could be produced in these deletions.

The  $\alpha$ PS2 residues encoded by exon 8 cause  $\alpha$ PS2C $\beta$ PS integrins to interact more effectively with Tigrin, as assessed by cell spreading [Zavortink et al., 1993; Graner et al., 1998] and TWOW-1 affinity. This might suggest that exon 8 residues contribute to specific contacts with Tigrin. However, the data showing that  $\alpha$ PS2m8-containing integrins become more like  $\alpha$ PS2C-containing integrins when activated by Mn<sup>2+</sup> ions and cytoplasmic domain mutations suggest an alternative hypothesis. The exon 8 sequences may function primarily to drive a conformational equilibrium to a state that is more conducive to Tigrin association, without directly interacting with the ligand. Of course, these two hypotheses are not mutually exclusive. In any case, all of the exon 8 variants described here, when activated by Mn<sup>2+</sup>, can bind similar amounts of TWOW-1 under saturating conditions, thus the changes do not eliminate structures that are required for ligand binding.

It is tempting to explain the m8-C difference in TWOW-1 binding as being due to the new

extensive loop in  $\alpha$ PS2C. However, the  $\alpha$ PS2m8-C subunit contains virtually all of this loop, and its TWOW-1 binding is much less than that seen for  $\alpha$ PS2C integrins. Another hypothesis is that the residues of the third  $\beta$  strand are critical. However, the two C-del variants each contain the  $\alpha$ PS2C strand sequence GQTYSI, but result in relatively low TWOW-1 affinity compared to  $\alpha$ PS2C. Thus, both the loop and strand appear to matter, but neither of these alone can fully or even mostly account for the m8-C difference. To summarize, for high levels of TWOW-1 binding the extra loop found in  $\alpha$ PS2C appears to be necessary, but not sufficient. Conversely, the benefits of the  $\alpha$ PS2C loop can largely be negated by incorporating the third  $\beta$  strand and immediately adjacent residues from  $\alpha$ PS2m8 (as seen for  $\alpha$ PS2m8-C).

Perhaps the most curious result derives from examination of Ca<sup>2+</sup> requirements for TWOW-1 binding and integrin-mediated cell spreading on Tigrin fragments.  $\alpha$ PS2C integrins perform well in both assays when Ca<sup>2+</sup> is depleted by saturating amounts of EGTA, but replacement of the  $\alpha$ PS2C isoleucine at the end of the  $\beta$  strand with the  $\alpha$ PS2m8 histidine (in C-H) is sufficient to restore most of the Ca<sup>2+</sup> requirement. Integrin  $\alpha$  subunits contain at least five potential Ca<sup>2+</sup> binding sites, four along the base of the  $\beta$ -propeller and a fifth at a flex point (the “genu”) in the stalk [Xiong et al., 2001]. None of these are obviously expected to be affected by exon 8 residues or the mutants described here, nor are there any data to indicate that these cation binding sites are important for integrin regulation. Much more work has been done to describe regulatory functions for the three cation binding sites of the  $\beta$  subunit A or I-like domain [Takagi et al., 2002; Xiong et al., 2002; Chen et al., 2003, 2004, 2006; Mould et al., 2003; Xiao et al., 2004; Arnaout et al., 2005; Pesho et al., 2006]. It is clear that the cation of the MIDAS domain interacts directly with the aspartate of RGD ligands, but there is no consensus opinion as to the roles of the flanking LIMBS and ADMIDAS sites, or for their cation binding specificities. What is clear is that cations in these sites can be important for modulating ligand binding and for propagating conformational changes through the integrin heterodimer.

The combined TWOW-1 affinity and Ca<sup>2+</sup> sensitivity data are most consistent with models in which the  $\alpha$ PS2C loop effects conformational

changes via a mechanism that requires a specific structure at the C-terminal end of the third  $\beta$  sheet strand of the third blade of the propeller. Additional homology modeling does not immediately suggest that the I > H replacement in  $\alpha$ PS2C-H will have significant effects on  $\alpha$  subunit structure (K. Shakalya and D. Mahadevan, unpublished work). However, one must remember that the X-ray data upon which our modeling is based are snapshots of structures that are stabilized in crystals of integrin fragments. Although our understanding of the gross features of integrin structure and function has advanced significantly in recent years, we are only beginning to uncover finer structural, and often dynamic, nuances that lie behind the exquisite functional details that characterize integrin biology. These blades of the  $\alpha$  subunit  $\beta$ -propeller are known to contain residues important in ligand binding [Irie et al., 1995, 1997; Kamata et al., 1996, 2001], and even minor alterations in the positioning of any residues in this region could alter binding.

Furthermore, it is not unreasonable to envision that changes in  $\alpha$  and  $\beta$  subunits, brought about by  $\alpha$ PS2 splicing variants and  $Mn^{2+}$ , respectively, would influence the  $\alpha/\beta$  interface in ways that would affect affinity for specific ligands, such as Tiggrin/TWOW-1, and which might be difficult to capture in structures of crystals of integrin fragments. It is very possible that the  $Ca^{2+}$  insensitivity of  $\alpha$ PS2C results from a change in  $\alpha/\beta$  contacts that can compensate for the requirement for cation binding to a  $\beta$  subunit site, and that an equilibrium involving these contacts can be influenced by a single residue that alters the conformation of the  $\alpha$ PS2  $\beta$ -propeller in subtle ways.

#### Similarities to Human $\alpha$ Subunits

Alternative splicing in the extracellular domains of vertebrate integrins is uncommon, but one example bears a remarkable similarity to that seen for  $\alpha$ PS2 [reviewed in de Melker and Sonnenberg, 1999]. In the identical position to the Drosophila exon 8, the human laminin receptor  $\alpha 6$  and  $\alpha 7$  genes have alternative exons denoted X1 and X2.  $\alpha 6$  utilizes either X1 or both X1 and X2; no functional differences between these have been noted, although there appears to be a preference of the  $\alpha 6X1X2$  isoform to associate with  $\beta 4$  instead of  $\beta 1$  [Delwel et al., 1995]. The largely muscle-specific  $\alpha 7\beta 1$  integrin has been studied more extensively. Unlike  $\alpha 6$ ,

$\alpha 7$  is found with X1 or X2-encoded residues, but not both [Ziober et al., 1993]. Like  $\alpha$ PS2m8,  $\alpha 7X1$  is most common where tissues are morphologically dynamic, whereas  $\alpha$ PS2C and  $\alpha 7X2$  are prevalent where stable cell-matrix adhesions are called for [Brown et al., 1989; Ziober et al., 1993; de Melker and Sonnenberg, 1999]. Cells expressing  $\alpha 7X1$  or  $\alpha 7X2$  show similar binding or motility properties on some laminins, but  $\alpha 7X2$  is superior on laminin 1 [Ziober et al., 1997; Schöber et al., 2000; von der Mark et al., 2002]. However,  $\alpha 7X1\beta 1$  can become an efficient laminin 1 receptor if cells are incubated with activating  $\beta 1$  antibodies or when  $\alpha 7X1$  is expressed with the muscle-specific  $\beta 1D$  cytoplasmic splice variant [Ziober et al., 1997; Yeh et al., 2003]. These data indicate that like the inclusion of exon 8 in  $\alpha$ PS2, the residues of the X1 and X2 exons of  $\alpha 7$  do not define cell adhesion specificities only by making specific ligand contacts directly, but also possibly by more global effects on integrin conformation.

#### ACKNOWLEDGMENTS

We wish to thank Barb Carolus and Debbie Sakiestewa of the Arizona Cancer Center Flow Cytometry Service for much assistance. Candida Morris and Alison Jannuzi assisted with manuscript preparation. Supported by Grants from the NIH to DLB (R01GM42474) and the American Cancer Society to DM (5P30CA023074).

#### REFERENCES

- Arnaut MA, Mahalingam B, Xiong JP. 2005. Integrin structure, allostery, and bidirectional signaling. *Annu Rev Cell Dev Biol* 21:381–410.
- Beglova N, Blacklow SC, Takagi J, Springer TA. 2002. Cysteine-rich module structure reveals a fulcrum for integrin rearrangement upon activation. *Nat Struct Biol* 9:282–287.
- Brower DL. 2003. Platelets with wings: The maturation of Drosophila integrin biology. *Curr Opin Cell Biol* 15:607–613.
- Brown NH, King DL, Wilcox M, Kafatos FC. 1989. Developmentally regulated alternative splicing of Drosophila integrin PS2  $\alpha$  transcripts. *Cell* 59:185–195.
- Brown NH, Gregory SL, Martin-Bermudo MD. 2000. Integrins as mediators of morphogenesis in Drosophila. *Dev Biol* 223:1–16.
- Bunch TA, Brower DL. 1992. Drosophila PS2 integrin mediates RGD dependent cell-matrix interactions. *Development* 116:239–247.
- Bunch TA, Miller SW, Brower DL. 2004. Analysis of the Drosophila  $\beta$ PS subunit indicates that regulation of integrin activity is a primal function of the C8-C9 loop. *Exp Cell Res* 294:118–129.

- Bunch TA, Helsten TL, Kendall TL, Shirahatti N, Mahadevan D, Shattil SJ, Brower DL. 2006. Amino acid changes in *Drosophila*  $\alpha$ PS2 $\beta$ PS integrins that affect ligand affinity. *J Biol Chem* 281:5050–5057.
- Burke RD. 1999. Invertebrate integrins: Structure, function, and evolution. *Int Rev Cytol* 191:257–284.
- Chen J, Salas A, Springer TA. 2003. Bistable regulation of integrin adhesiveness by a bipolar metal ion cluster. *Nat Struct Biol* 10:995–1001.
- Chen J, Takagi J, Xie C, Xiao T, Luo BH, Springer TA. 2004. The relative influence of metal ion binding sites in the I-like domain and the interface with the hybrid domain on rolling and firm adhesion by integrin  $\alpha$ 4 $\beta$ 7. *J Biol Chem* 279:55556–55561.
- Chen J, Yang W, Kim M, Carman CV, Springer TA. 2006. Regulation of outside-in signaling and affinity by the  $\beta$ 2 I domain of integrin  $\alpha$ L $\beta$ 2. *Proc Natl Acad Sci USA* 103:13062–13067.
- de Melker AA, Sonnenberg A. 1999. Integrins: Alternative splicing as a mechanism to regulate ligand binding and integrin signaling events. *BioEssays* 21:499–509.
- Delwel GO, Kuikman I, Sonnenberg A. 1995. An alternatively spliced exon in the extracellular domain of the human  $\alpha$ 6 integrin subunit-functional analysis of the  $\alpha$ 6 integrin variants. *Cell Adhes Commun* 3:143–161.
- Fogerty FJ, Fessler LI, Bunch TA, Yaron Y, Parker CG, Nelson RE, Brower DL, Gullberg D, Fessler JH. 1994. Tigrin, a novel *Drosophila* extracellular matrix protein that functions as a ligand for *Drosophila*  $\alpha$ PS2 $\beta$ PS integrins. *Development* 120:1747–1758.
- Graner MW, Bunch TA, Baumgartner S, Kerschen A, Brower DL. 1998. Splice variants of the *Drosophila* PS2 integrins differentially interact with RGD-containing fragments of the extracellular proteins tigrin, ten-m, and D-laminin 2. *J Biol Chem* 273:18235–18241.
- Hynes RO. 2002. Integrins: Bidirectional allosteric signaling machines. *Cell* 110:673–687.
- Hynes RO, Zhao Q. 2000. The evolution of cell adhesion. *J Cell Biol* 150:F89–F95.
- Irie A, Kamata T, Puzon-McLaughlin W, Takada Y. 1995. Critical amino acid residues for ligand binding are clustered in a predicted  $\beta$ -turn of the third N-terminal repeat in the integrin  $\alpha$ 4 and  $\alpha$ 5 subunits. *EMBO J* 14:5550–5556.
- Irie A, Kamata T, Takada Y. 1997. Multiple loop structures critical for ligand binding of the integrin  $\alpha$ 4 subunit in the upper face of the  $\beta$ -propeller model. *Proc Natl Acad Sci USA* 94:7198–7203.
- Jannuzi AL, Bunch TA, Brabant MC, Miller SW, Mukai L, Zavortink M, Brower DL. 2002. Disruption of C-Terminal cytoplasmic domain of  $\beta$ PS integrin subunit has dominant negative properties in developing *Drosophila*. *Mol Biol Cell* 4:1352–1365.
- Jin M, Andricioaei I, Springer TA. 2004. Conversion between three conformational states of integrin I domains with a C-terminal pull spring studied with molecular dynamics. *Structure* 12:2137–2147.
- Kamata T, Irie A, Tokuhira M, Takada Y. 1996. Critical residues of integrin  $\alpha$ IIB subunit for binding of  $\alpha$ IIB $\beta$ 3 (glycoprotein IIb-IIIa) to fibrinogen and ligand-mimetic antibodies (PAC-1, OP-G2, and LJ-CP3). *J Biol Chem* 271:18610–18615.
- Kamata T, Tieu KK, Irie A, Springer TA, Takada Y. 2001. Amino acid residues in the  $\alpha$ IIB subunit that are critical for ligand binding to integrin  $\alpha$ IIB $\beta$ 3 are clustered in the  $\beta$ -propeller model. *J Biol Chem* 276:44275–44283.
- Litvinov RI, Bennett JS, Weisel JW, Shuman H. 2005. Multi-step fibrinogen binding to the integrin  $\alpha$ IIB $\beta$ 3 detected using force spectroscopy. *Biophys J* 89:2824–2834.
- Liu S, Calderwood DA, Ginsberg MH. 2000. Integrin cytoplasmic domain binding proteins. *J Cell Sci* 113:3563–3571.
- Luo B-H, Springer TA. 2006. Integrin structures and conformational signaling. *Curr Opin Cell Biol* 18:1–8.
- Luo B-H, Springer TA, Takagi J. 2003. Stabilizing the open conformation of the integrin headpiece with a glycan wedge increases affinity for ligand. *Proc Natl Acad Sci USA* 100:2403–2408.
- Mould AP, Humphries MJ. 2004. Regulation of integrin function through conformational complexity: Not simply a knee-jerk reaction? *Curr Opin Cell Biol* 16:544–551.
- Mould AP, Barton SJ, Askari JA, Craig SE, Humphries MJ. 2003. Role of ADMIDAS cation-binding site in ligand recognition by integrin  $\alpha$ 5 $\beta$ 1. *J Biol Chem* 278:51622–51629.
- Pampori N, Hato T, Stupack DG, Aidoudi S, Cheresh DA, Nemerow GR, Shattil SJ. 1999. Mechanisms and consequences of affinity modulation of integrin  $\alpha$ v $\beta$ 3 detected with a novel patch-engineered monovalent ligand. *J Biol Chem* 274:21609–21616.
- Pesho MM, Bledzka K, Michalec L, Cierniewski CS, Plow EF. 2006. The specificity and function of the metal-binding sites in the integrin  $\beta$ 3 A-domain. *J Biol Chem* 281:23034–23041.
- Schöber S, Mielenz D, Echtermeyer F, Hapke S, Pöschl E, von der Mark H, Moch H, von der Mark K. 2000. The role of extracellular and cytoplasmic splice domains of  $\alpha$ 7-integrin in cell adhesion and migration on laminins. *Exp Cell Res* 255:303–313.
- Springer TA. 1997. Folding of the N-terminal, ligand-binding region of integrin  $\alpha$ -subunits into a  $\beta$ -propeller domain. *Proc Natl Acad Sci USA* 94:65–72.
- Springer TA, Wang JH. 2004. The three-dimensional structure of integrins and their ligands, and conformational regulation of cell adhesion. *Adv Protein Chem* 68:29–63.
- Takagi J, Petre BM, Walz T, Springer TA. 2002. Global conformational rearrangements in integrin extracellular domains in outside-in and inside-out signaling. *Cell* 110:599–611.
- von der Mark H, Williams I, Wendler O, Sorokin L, von der Mark K, Pöschl E. 2002. Alternative splice variants of  $\alpha$ 7 $\beta$ 1 integrin selectively recognize different laminin isoforms. *J Biol Chem* 277:6012–6016.
- Xiao T, Takagi J, Collier BS, Wang JH, Springer TA. 2004. Structural basis for allostery in integrins and binding to fibrinogen-mimetic therapeutics. *Nature* 432:59–67.
- Xiong J-P, Stehle T, Diefenbach B, Zhang R, Dunker R, Scott DL, Joachimiak A, Goodman SL, Arnaout MA. 2001. Crystal structure of the extracellular segment of integrin  $\alpha$ v $\beta$ 3. *Science* 294:339–345.
- Xiong J-P, Stehle T, Zhang R, Joachimiak A, Frech M, Goodman SL, Arnaout MA. 2002. Crystal structure of the extracellular segment of integrin  $\alpha$ v $\beta$ 3 in complex with an arg-gly-asp ligand. *Science* 296:151–155.
- Xiong J-P, Stehle T, Goodman SL, Arnaout MA. 2003. Integrins, cations and ligands: Making the connection. *J Thromb Haemost* 1:1642–1654.

- Yeh M-G, Ziober BL, Liu B, Lipkina G, Vizirianakis IS, Kramer RH. 2003. The  $\beta 1$  cytoplasmic domain regulates the laminin-binding specificity of the  $\alpha 7 X 1$  integrin. *Mol Biol Cell* 14:3507–3518.
- Zavortink M, Bunch TA, Brower DL. 1993. Functional properties of alternatively spliced forms of the Drosophila PS2 integrin  $\alpha$  subunit. *Cell Adhes Commun* 1:251–264.
- Ziober BL, Vu MP, Waleh N, Crawford J, Lin C-S, Kramer RH. 1993. Alternative extracellular and cytoplasmic domains of the integrin  $\alpha 7$  subunit are differentially expressed during development. *J Biol Chem* 268:26773–26783.
- Ziober BL, Chen Y, Kramer RH. 1997. The laminin-binding activity of the  $\alpha 7$  integrin receptor is defined by developmentally regulated splicing in the extracellular domain. *Mol Biol Cell* 8:1723–1734.